molecular pharmaceutics

Article

pubs.acs.org/molecularpharmaceutics

Targeting to Endothelial Cells Augments the Protective Effect of Novel Dual Bioactive Antioxidant/Anti-Inflammatory Nanoparticles

Melissa D. Howard,[†] Elizabeth D. Hood,[†] Colin F. Greineder,[†,‡] Ivan S. Alferiev,[§,∥] Michael Chorny,[§,∥] and Vladimir Muzykantov*[,†]

[†]Department of Pharmacology and Center for Targeted Therapeutics and Translational Nanomedicine, Perelman School of Medicine, University of Pennsylvania, Philadelphia, Pennsylvania 19104, United States

[‡]Department of Emergency Medicine, Perelman School of Medicine, University of Pennsylvania, Philadelphia, Pennsylvania 19104, United States

[§]Division of Cardiology, Abramson Research Center, The Children's Hospital of Philadelphia, Philadelphia, Pennsylvania 19104, United States

[∥]Department of Pediatrics, Perelman School of Medicine, University of Pennsylvania, Philadelphia, Pennsylvania 19104, United States

Supporting Information

ABSTRACT: Oxidative stress and inflammation are intertwined contributors to numerous acute vascular pathologies. A novel dual bioactive nanoparticle with antioxidant/anti-inflammatory properties was developed based on the interactions of tocopherol phosphate and the manganese porphyrin SOD mimetic, MnTMPyP. The size and drug incorporation efficiency were shown to be dependent on the amount of MnTMPyP added as well as the choice of surfactant. MnTMPyP was shown to retain its SOD-like activity while in intact particles and to release in a slow and controlled manner. Conjugation of anti-PECAM antibody to the nanoparticles provided endothelial targeting and potentiated nanoparticle-mediated suppression of inflammatory activation of these cells manifested by expression of VCAM, E-selectin, and IL-8. This nanoparticle technology may find applicability with drug combinations relevant for other pathologies.

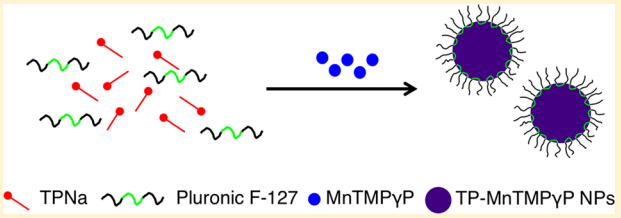

KEYWORDS: *inflammation, oxidative stress, SOD mimetic, nanocarrier, ROS, tocopherol, cytokines, targeted drug delivery, nanoparticles, antioxidants/anti-inflammatory, tocopherol/vitamin E, endothelial cells*

INTRODUCTION

Nanoparticles (NPs) have numerous advantages as drug delivery carriers, including enhanced drug solubility and stability, targeting ability, and controlled drug release. One recent area of interest is the design of nanoparticles that deliver multiple drugs simultaneously. Clinically, use of multiple drugs is the standard of care for treatment of most diseases. Drugs can be administered that target multiple pathways or that are designed to act sequentially. Ideally, the result is additive or even synergistic effects.[1,2] Ensuring that target cells receive both drugs in comparison to just one (as might happen if drugs or nanoparticles are just administered concomitantly) may also prove beneficial.[3]

The concept of multidrug carriers has mostly been explored with chemotherapeutic agents to date. Pharmacological management of acute vascular inflammation and oxidative stress represents an alternative scenario where this drug delivery approach may be highly advantageous. Reactive oxygen species (ROS) have been implicated as both injurious and proinflammatory signaling agents in vascular pathology.[4−6] In particular, endothelial cells that form the interphase monolayer lining the luminal surface of blood vessels represent the key therapeutic site for antioxidant and anti-inflammatory interventions in acute pathological conditions, including ischemia/reperfusion and endotoxemia.[7−10]

In the pathogenesis of these conditions [e.g., stroke, ischemia/reperfusion (I/R), acute lung injury (ALI)], proinflammatory factors induce activation of endothelial NADPH oxidase (Nox), triggering a flux of superoxide anion (O_2^-) into the intracellular region.[11,12] Specifically, endosomal O_2^- is known to activate the inflammatory NF-κB pathway, leading to the expression of inducible adhesion molecules (e.g., VCAM-1),[13] enhanced permeability,[14] and loss of the antithrombotic phenotype.[15] This leads to tissue injury and further aggravation and perpetuation of the inflammatory cycle.[16] Therefore, both oxidative and proinflammatory pathways are intertwined and mutually propagate each other, providing an impetus for codelivery of antioxidants and anti-inflammatory agents for treatment of acute inflammatory vascular pathologies.

This paper reports on a novel NP formulation, where two bioactive compounds, tocopherol phosphate (TP) and Mn-

Received: November 9, 2013
Revised: April 7, 2014
Accepted: May 30, 2014
Published: May 30, 2014

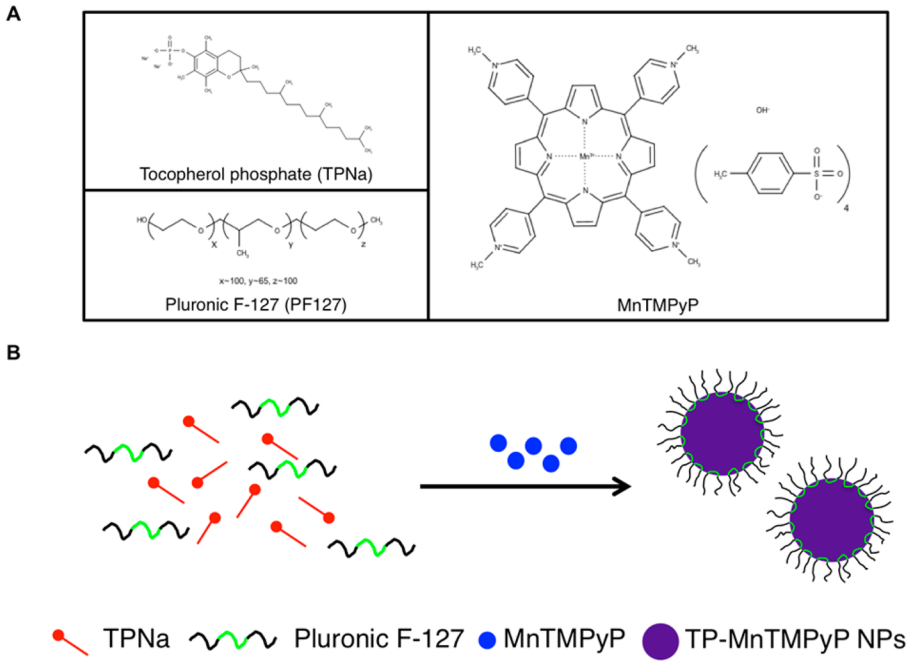

Figure 1. (A) Structures of TPNa, MnTMPyP, and PF127. (B) Schematic of colloidal aggregation and precipitation procedure used for the preparation of bioactive NPs.

(III)tetrakis(1-methyl-4-pyridyl)porphyrin (MnTMPyP), are combined to form an ion-pair complex that also acts as the structural particle-forming material. The two components exhibit complementary, but not identical, biological activities. Whereas MnTMPyP is a manganese porphyrin superoxide dismutase (SOD) mimetic with strong antioxidant effects,[17,18] TP—the phosphate derivative of the α-tocopherol form of vitamin E—is thought to function primarily as an anti-inflammatory signaling agent. Several studies have reported TP to have activity independent of and surpassing of α-tocopherol, including reducing expression of inflammatory biomarkers,[19] inhibiting cell proliferation,[20,21] and increasing angiogenesis.[20] Combining these two drugs creates the potential for synergistic biological activity and simultaneously allows the particle properties to be readily controlled by adjusting the ratio between the constituent pharmacophores. The net effect is a NP with significant advantages from both pharmacologic and pharmaceutical standpoints (Figure 1).

While TP is highly water-soluble in its sodium salt form, its precipitation in the form of small, uniformly sized NPs when combined with MnTMPyP in the presence of a surfactant, generally Pluronic F-127 (PF127), obviates the need for incorporating biologically inactive excipients (e.g., lipids, polymers). This in turn greatly enhances the therapeutic payload of the formulation and reduces the dose required for achieving a therapeutically adequate effect, potentially enhancing the translation of these nanocarriers for clinical use.

For endothelial targeting, antibodies to the endothelial cell surface determinant platelet endothelial cell adhesion molecule, PECAM-1, were attached to the surface of the NPs. PECAM is constitutively expressed on the surface of endothelial cells at a level of $\sim 1 \times 10^6$ copies/cell.[22] Nanocarriers and proteins conjugated to anti-PECAM have previously been shown to be delivered to endothelial cells in vitro and in intact animals.[23,24] Antioxidants delivered to endothelial cells using such PECAM-targeted carriers exert protective effects in cell culture and animal models of acute ROS-mediated endothelial pathology.[25−27]

MATERIALS AND METHODS

Reagents. TPNa, D-α-tocopherol poly(ethylene glycol) 1000 succinate (TPGS), PF127, 1,3-dicyclohexylcarbodiimide (DCC), 2,6-di-*tert*-butyl-*p*-cresol (BHT), and methanol were purchased from Sigma-Aldrich (St. Louis, MO). MnTMPyP was from Calbiochem (EMD Millipore, Billerica, MA). 6-Maleimidohexanoic acid was from AK Scientific (Union City, CA). Succinimidyl 4-[*N*-maleimidiomethyl]cyclohexane-1-carboxylate (SMCC) and *N*-succinimidyl *S*-acetylthioacetate (SATA) were from Thermo Scientific Pierce (Rockford, IL). Streptavidin was from Calbiochem (San Diego, CA). Mouse anti-PECAM MEC13.3 was purchased from BD Bioscience (San Jose, CA), and monoclonal antibody (mAb 62) against human anti-PECAM was provided by Dr. Marian Nakada (Centoor; Malvern, PA). Whole molecule rat IgG was from Rockland Immunochemicals (Gilbertsville, PA).

Preparation of Pluronic F-127 Biotin. The biotinylation of the triblock copolymer Pluronic F-127 took place in several steps (Scheme 1 in the Supporting Information). First, Pluronic F-127 in $CHCl_3$ was reacted with a large excess of tosyl chloride (TsCl) in the presence of triethylamine in an atmosphere of argon at room temperature. The tosylated polymer was coarsely purified from triethylamine hydrochloride via filtration of toluene solution, and from the excess of TsCl using several precipitations with hexane. The resulting tosylated polymer was reacted with potassium salt of phthalimide in DMF solution at 80−90 °C for 3 h. The phthalimide-modified polymer was coarsely separated from nonpolymeric impurities by dissolution in toluene and filtration through a pad of microgranular cellulose. The polymer was purified on a column with silica gel (eluent $CHCl_3$/MeOH, 1:0 to 1:0.5). Complete modification of the terminal hydroxyl groups was verified by ^{1}H NMR. The modified polymer was then cleaved using a standard procedure (reflux for 2 h with hydrazine hydrate in EtOH followed by

dx.doi.org/10.1021/mp400677y | *Mol. Pharmaceutics* 2014, 11, 2262−2270

removal of the excess hydrazine in vacuum and acidification with HCl). The amino-terminated Pluronic F-127 was dissolved in CH_2Cl_2, freed from insoluble impurities by filtration through microgranular cellulose, and finally purified on a column with silica gel (eluent $CHCl_3$/MeOH, 30:1 to 1:0.5). The hydrochloride form of the polymer was transformed into the free base by treatment with a large excess of Na_2CO_3 in water/MeOH/*i*-PrOH. ^{1}H NMR (400 MHz, $CDCl_3$) of the amino-terminated Pluronic F-127 exhibited NH_2-bound CH_2 at δ 2.83 and no signals of uncleaved phthalimide residues. The amino-terminated Pluronic F-127 was reacted with biotin *N*-succinimidyl ester as shown in the final step of Scheme 1 in the Supporting Information.

Preparation of Pluronic F-127 Maleimide. Pluronic F-127 in CH_2Cl_2 was reacted with 6-maleimidohexanoic acid and DCC for 3.5 h at room temperature in the presence of BHT, which was added to prevent polymerization. After filtering off the precipitate of 1,3-dicyclohexylurea, the crude polymer was precipitated with hexane (removing the excess of DCC) and purified by flash chromatography (silica gel, $CHCl_3$−methanol, 100:0 to 4:1) (Scheme 2 in the Supporting Information). ^{1}H NMR of the modified polymer (400 MHz, $CDCl_3$) detected the signal of maleimide protons at δ 6.67 ppm, whereas the signal of terminal CH_2OH at δ 2.78 ppm disappeared, indicating the completeness of derivatization.

Cell Culture. Human umbilical vein endothelial cells (HUVECs) were purchased at first passage from Lonza Walkersville (Walkersville, MD) and grown in Falcon tissue culture flasks (BD Biosciences, San Jose, CA) coated with 1% gelatin (Becton, Dickinson and Company; Sparks, MD). EGM-BulletKit medium (Lonza Walkersville) containing 10% v/v fetal bovine serum (FBS) was used. All studies were performed with passage 5 cells in a confluent state (5×10^4 cells/cm^2).

NP Preparation. All solutions were prepared in Tris buffer (50 mM). Fifty microliters of 10% TPNa and surfactant (10% and PF127 unless stated otherwise) were mixed. MnTMPyP (50 μL of the appropriate concentration) was then added dropwise to that solution with stirring. To enable antibody conjugation, 5 μL of the 10% PF127 solution could be substituted with either 10% PF127-biotin or 10% PF127-maleimide. Purification of the formed particles was performed using a Sepharose CL-4B gel filtration column (Sigma-Aldrich). If necessary, samples were reconcentrated by ultrafiltration (10k MWCO, Amicon centrifugal filter units, EMD Millipore) in the presence of 5% sucrose.

Antibody-SATA (Ab-SATA) Modification. Antibodies were modified with SATA in a manner similar to that previously described.[13] Briefly, SATA was added to the Ab in a 10-fold molar excess for 30 min at room temperature in order to introduce ∼1 sulfhydryl group per Ab. *N*-Hydroxylamine (0.5 M) was then added at a 1:10 volume ratio for 2 h in order to deprotect acetylated sulfhydryls. Zeba desalting columns (Thermo Scientific Pierce) were used to remove unreacted components at each step of the process.

Antibody-SA (Ab-SA) Conjugate Preparation. Ab was modified with SATA as described above, but using a 6:1 molar ratio SATA:Ab. In a parallel reaction, stable maleimide groups were introduced onto SA using a 20-fold molar excess of SMCC at room temperature for 1 h. Again, products were passed through desalting columns for the removal of unreacted components. Streptavidination of the Ab was achieved using a 2:1 molar ratio Ab:SA in a 1 h reaction on ice.

Surface Coating of NPs with Modified Antibodies. NPs prepared with PF127-maleimide and PF127-biotin were coated with Ab-SATA and Ab-SA, respectively. NPs and modified antibodies were mixed for 5 min at room temperature (longer times did not show enhanced antibody conjugation, unpublished data). As mentioned above, a Sepharose CL-4B gel filtration column was used for removal of free drug and antibody. Binding efficiency was measured by radiotracing a 10% substitution of ^{125}I-IgG-SATA or ^{125}I-IgG-SA. A *t* test (two-tail, homoscedastic) was used to compare conjugation chemistries; a *p*-value of 0.05 was considered statistically significant.

Antibody radiolabeling was performed using iodination beads as instructed by the manufacturer (Pierce Iodination Beads, Thermo Scientific, Pittsburgh, PA). The extent of radiolabeling was measured using a standard trichloroacetic acid (TCA) assay. Two microliters of labeled antibody, 1 mL of 3% BSA, and 200 μL of TCA were mixed and incubated at room temperature for 15 min. Following centrifugation (15 min, 4 °C, 2300*g*), the amount of free iodine in the supernatant was quantified using a Wizard^2 2470 gamma counter (PerkinElmer; Waltham, MA).

Analytical Methods. Size and polydispersity index (PDI) were measured by dynamic light scattering using a 90Plus Particle Size Analyzer (Brookhaven Instruments, Holtsville, NY) following a 10-fold dilution in deionized (DI) H_2O. UV measurements were performed on a Varian Cary 50 Bio UV−visible spectrophotometer (Agilent Technologies, Santa Clara, CA). MnTMPyP concentration was calculated based on a standard curve obtained at 460 nm from 1 to 20 μM in DI H_2O. Incorporation efficiency was calculated as incorporated drug/added drug × 100. Measurements were obtained for initial NP preparations, purified NPs, and free material to confirm ∼100% drug recovery. Particle breakdown was achieved using a 1:2 dilution with 0.5 M EDTA prior to dilution with DI H_2O.

TPNa concentration was assessed using a Waters HPLC system equipped with a Nova-Pak C18 (3.9 × 150 mm, 4 μm) column. The mobile phase was 95% MeOH/5% H_2O run at 0.5 mL/min. Concentration was calculated based on a standard curve obtained at 290 nm from 10 to 1000 μg/mL. Encapsulation efficiency was calculated as described above. NP samples were treated with EDTA (to disrupt particle structure) and NaCl (to convert tocopherol phosphate back to sodium salt form) in a concentration-dependent manner prior to dilution with MeOH.

The SOD-like activity of MnTMPyP was determined using a cytochrome C reduction assay in which xanthine and xanthine oxidase are combined to produce superoxide anion and cytochrome C acts as an indicating scavenger that competes with the mimetic. The working solution (0.6 mL) contained 50 mM phosphate buffer (pH 7.8), 0.1 mM EDTA, 20 μM cytochrome C, and 50 μM xanthine. Reaction was initiated by the addition of 10 μL of 0.2 U/mL xanthine oxidase, and the absorbance was monitored at 550 nm. A one-way ANOVA was performed to provide comparison among free MnTMPyP, intact particles, and EDTA-disrupted particles. A *p*-value of 0.05 was considered statistically significant.

Drug Release and Stability. Purified IgG-coated NPs substituted with 10% ^{125}I-IgG (1.5 mL) were loaded to 10 kDa MWCO Slide-a-lyzer dialysis cassettes (0.5−3 mL, Thermo Scientific) and dialyzed against either 200 mL of PBS or phosphate buffer (PB, 10 mM, pH 7.4) at 37 °C. At each time

point, 200 μL was removed from inside the cassette for measurement of size and remaining MnTMPyP. To correct for any dilution, the ^{125}I-IgG activity of a 10 μL aliquot was also measured at each time point and compared to the initial starting activity.

Binding of NPs to Endothelial Cells. Antibodies were conjugated using biotin−streptavidin chemistry and comparisons were made between targeted anti-PECAM and control IgG coated NPs. Cold antibodies were doped with 10% ^{125}I-IgG-SA for radiotracing. Use of this doping technique allows quantitative measurement of binding to cells while minimizing the chance of false positive results, such as might occur due to binding of detached Ab-SA if it was labeled directly. Cells were incubated with increasing quantities of NPs for 30 min at 37 °C. After the incubation, medium was removed, and the cells were lysed using 1% Triton X100 in 1 N NaOH. The radioactivity of both supernatants and cell lysates was measured. Particle number bound per cell calculations were derived on the basis of a NP concentration of 1×10^{13} particles/mL and an EC density of 10^5 cells/well on a 24 well plate.

Inflammatory Marker Expression by Quantitative PCR. HUVECs in 24 well plates were used at confluency (~10^5 cells/well). Anti-PECAM or IgG-coated NPs were added in fresh medium; control wells received medium alone. Following a 30 min incubation, medium was removed, and TNF (10 ng/mL in medium) was added. Medium was replaced in control wells. After 2.5 h of TNF exposure, medium was removed and cells were lysed in 350 μL of buffer RLT. Total cellular RNA was extracted using the RNeasy Mini Kit (Qiagen, Valencia, CA) according to the manufacturer's instructions. cDNA was synthesized using the High Capacity cDNA Reverse Transcription Kit, and qPCR was performed using Fast SYBR Green Master Mix and a ViiA 7 system (Life Technologies, Grand Island, NY). Gene specific primers for human VCAM-1, E-selectin, and IL-8 were utilized as well as validated Quantitect primers for 18S rRNA and GAPDH (Qiagen).[28] Relative gene expression was quantified using the comparative C_T method, using 18S rRNA and GAPDH as internal controls.[29] Comparisons were made by *t* test (two-tail, homoscedastic), and results were considered statistically significant at $p = 0.05$.

VCAM Expression by Western Blot. The study was performed as described above for PCR but with a 5 h TNF exposure. Cells were lysed in 100 μL of sample buffer for sodium dodecyl sulfate polyacrylamide gel electrophoresis. Samples were incubated at 100 °C for 5 min and then stored at 4 °C until use. Cell proteins were run on a 4−15% gradient gel (Biorad Laboratories, Hercules, CA) and transferred to a PVDF membrane (Millipore, Billerica, MA) for Western blotting. The membrane was subsequently blocked for 1 h with 3% nonfat dry milk in TBS-T (100 mM Tris, pH 7.6; 150 mM NaCl; and 0.1% Tween 20), followed by incubations with primary and secondary antibodies for VCAM and actin. The blot was detected using ECL Plus reagents (GE Healthcare, New York, NY). Quantification of blots was performed using standard densitometry methods (Biorad Fluor-SM, Biorad Laboratories, Hercules, CA). Comparisons were made by *t* test (two-tail, homoscedastic), and results were considered statistically significant at $p = 0.05$.

RESULTS

Effect of MnTMPyP on Size and Drug Loading. Dual bioactive NPs (PDI < 0.3) could be formed through mixing the soluble tocopherol phosphate sodium salt and MnTMPyP in the presence of a surfactant. As the concentration of MnTMPyP was increased, the incorporation of both components into particles increased (Figure 2A,B). The

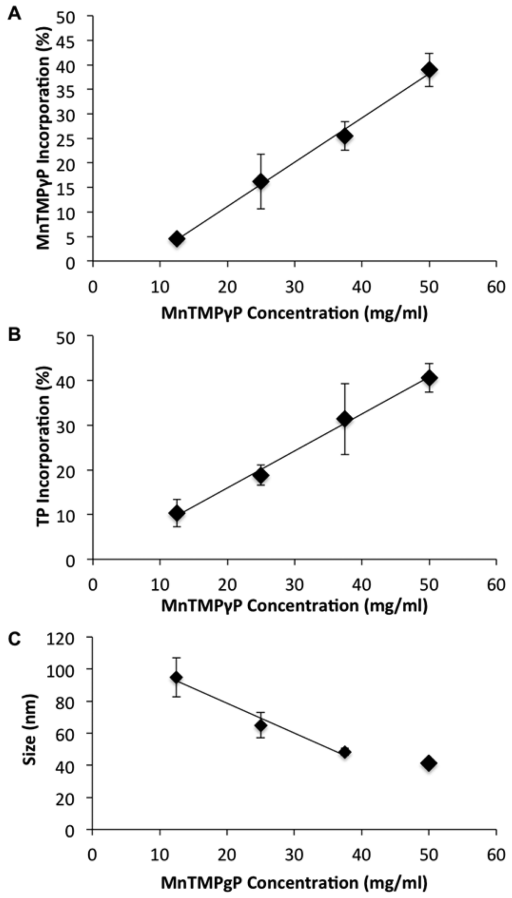

Figure 2. Effect of added MnTMPyP on NP incorporation of MnTMPyP (A), incorporation of TP (B), and size (C) (mean ± SD, $n = 3$).

increase was linear in both cases and similar numerically. As an example, with a concentration of 50 mg/mL MnTMPyP, corresponding to the MnTMPyP:TP molar ratio of 1:5, the loading for both drugs was around 40%. With a +5 charge for the MnTMPyP and a −2 charge for the TP (when both are in their free form), the 1:5 ratio observed indicates that displacement of the respective counterions was likely incomplete.

In contrast to the increase in drug loading, the size of the particles decreased as additional MnTMPyP was added (Figure 2C). This decrease appeared linear up to a MnTMPyP concentration of 37.5 mg/mL. Beyond a MnTMPyP concentration of 50 mg/mL, the formation of large aggregates was observed, and thus, higher drug concentrations were not pursued. Based on this data, a concentration of 50 mg/mL was chosen as the standard for further studies.

Effect of Surfactant Type and Concentration on Drug Loading. Changing the PF127 concentration had an insignificant effect on drug loading (Figure 3A,B). At a 50 mg/mL concentration, loading of both MnTMPyP and TP remained around 40% independent of whether 5, 10, or 20% PF127 was used in the starting preparation. There was a slight

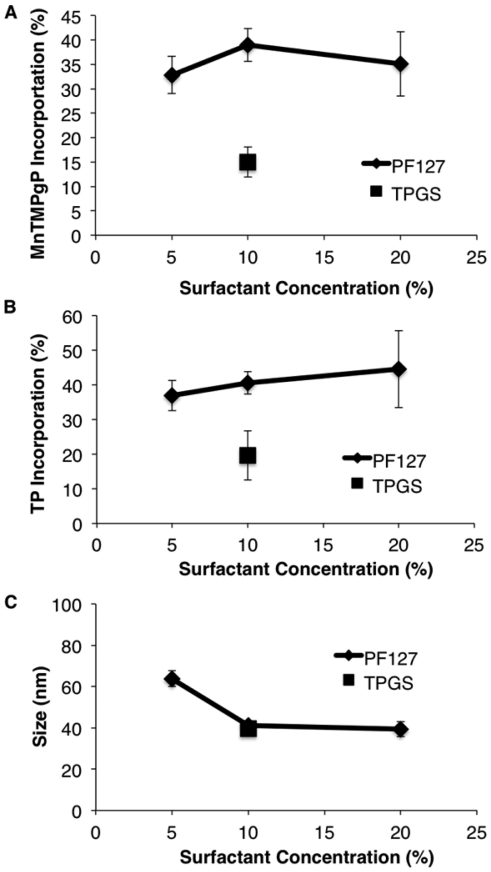

Figure 3. Effect of surfactant concentration on MnTMPyP incorporation (A), TP incorporation (B), and size (C) (mean ± SD, n = 3).

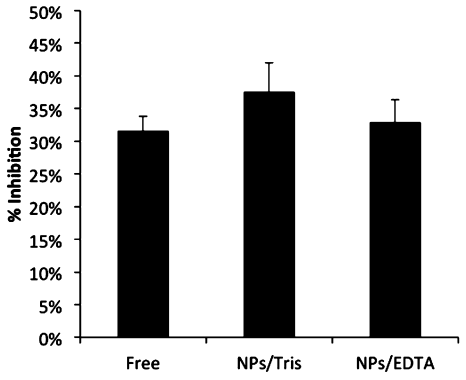

Figure 4. SOD-like activity of MnTMPyP (as measured by inhibition of cytochrome C reduction) when measured in its free form, in the intact particles (diluted in Tris buffer), or in EDTA-disrupted particles. There was no significant difference among the three samples (p = 0.361) (mean ± SD, n = 3).

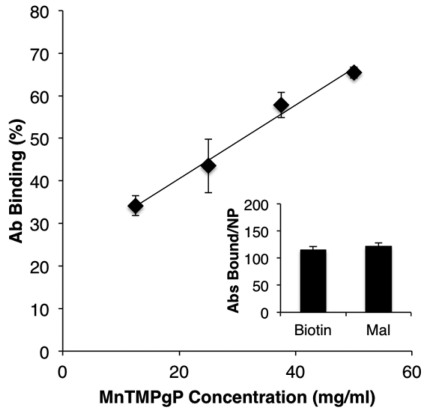

Figure 5. Effect of added MnTMPyP on antibody binding to NPs. (inset) Comparison of antibody binding chemistries on total antibodies bound per NP. There was no significant difference in binding between the two chemistries (p = 0.258) (mean ± SD, n = 3).

decrease in size on going from 5% to 10% PF127 but no further drop on increasing to 20% PF127 (Figure 3C).

Interestingly, when 10% TPGS was used as a surfactant in lieu of 10% PF127, there was a large drop in incorporation efficiency of both MnTMPyP (from 40% to 15%) and TP (from 40% to 20%) (Figure 3A,B). Size, however, remained similar (Figure 3C).

SOD Activity. The SOD-like activity of MnTMPyP, as measured by inhibition of cytochrome C reduction by superoxide, was measured in its free form, in the intact particles, and in disrupted particles (Figure 4). When diluted to the same concentration, there was no significant difference among the three samples (p = 0.361 by one-way ANOVA).

Antibody Binding. Similar to drug encapsulation efficiency, the percentage of binding of antibodies to the NPs was shown to increase linearly with increasing MnTMPyP concentration (Figure 5). At the highest drug concentration, and hence maximum binding, a surface coating of ∼120 Abs/NP could be achieved when aiming for 200 Abs/NP. This was independent of the binding chemistry used: both biotin−streptavidin and SATA/SMCC conjugation techniques resulted in similar Ab surface coverage (Figure 5). A t test revealed no significant difference between the two samples (p = 0.258). NP size increased slightly (∼20 nm) with Ab binding, while PDI values remained similar (data not shown).

Drug Release and Stability. NPs were evaluated for release of MnTMPyP and change in size during incubation at 37 °C. As these particles are based highly on electrostatic interactions, comparisons were made between samples incubated in PBS versus those in a phosphate buffered solution alone. Drug release was accelerated in PBS as compared to phosphate buffer (PB), reaching ∼60% released at 24 h versus only 20% in PB alone (Figure 6A). There was a statistically significant difference in drug release at all time points following the initial one. However, the overall rate of drug release was still relatively slow. In contrast, the size of NPs remained constant throughout the entire time period and did not vary with the choice of diluent (Figure 6B). In agreement with drug dissociation observed in the absence of changes in the size of remaining particles, the number of particles was progressively decreasing as could be determined based on the counts reported in the course of DLS measurements (data not shown).

Cell Binding and Anti-Inflammatory Effect of Targeted NPs. HUVECs were used for characterizing the targeting ability of NPs. Targeted but not control IgG-coated NPs bound to the endothelial cells in a dose-dependent manner (Figure 7A). At the maximal dose, delivery of approximately 7,500 NPs per cell could be achieved within the first 30 min of exposure.

The enhanced targeting ability corresponded to an improved functional effect in this experimental model. Anti-PECAM NPs protected against the proinflammatory endothelial activation manifested by a variety of inflammatory markers (VCAM, E-selectin, and IL-8) as determined by PCR (Figure 7B). By t

dx.doi.org/10.1021/mp400677y | Mol. Pharmaceutics 2014, 11, 2262−2270

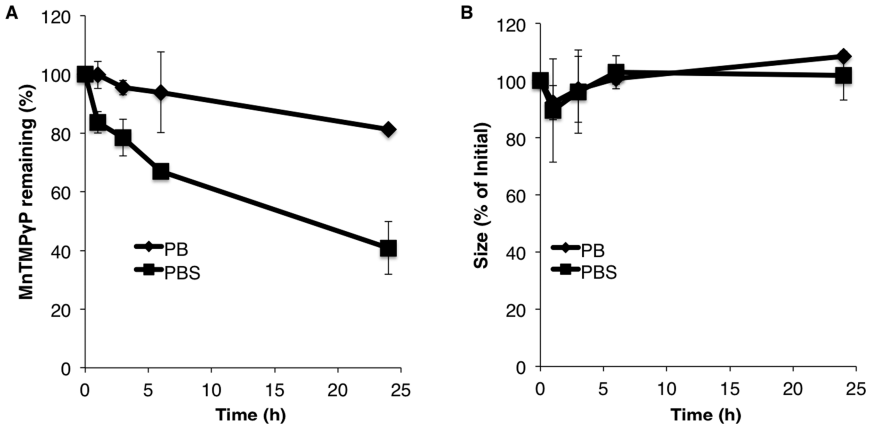

Figure 6. Drug release (A) and size stability (B) of NPs incubated at 37 °C (mean ± SD, n = 3).

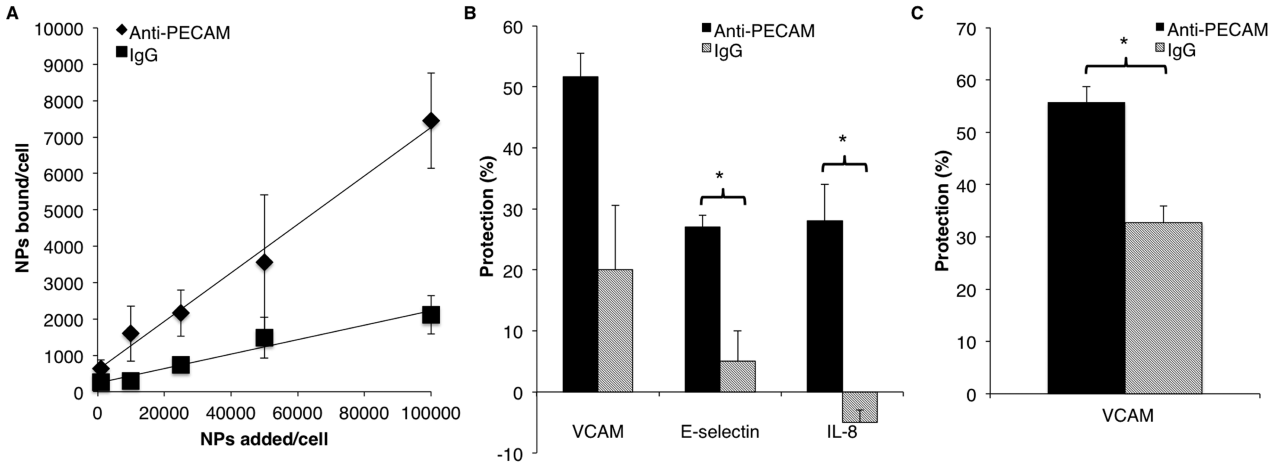

Figure 7. (A) HUVEC binding of PECAM targeted NPs versus control IgG NPs following a 30 min incubation. (B) Protection against proinflammatory endothelial activation as assessed by VCAM, E-selectin, and IL-8 RNA gene expression. (C) Protection against proinflammatory endothelial activation as assessed by upregulated VCAM protein levels (mean ± SD, n = 3, significance $p < 0.05$).

test, there was a statistically significant improvement of anti-inflammatory effect of targeted anti-PECAM vs control IgG coated NPs for E-selectin (p = 0.029) and IL-8 (p = 0.017) and a clear trend for VCAM (but not statistically significant, p = 0.057). The difference in effect between targeted and untargeted NPs was more pronounced with E-selectin and IL-8 through the whole dose range of NPs evaluated (Figure 1 in the Supporting Information).

Based on the significant augmentation of the protective effect of targeted vs nontargeted NP observed with VCAM transcription, an additional study was performed to evaluate this on the level of VCAM protein expression. Anti-PECAM NPs resulted in nearly 60% protection against the stimulation of VCAM synthesis (Figure 7C, Figure 2 in the Supporting Information). This was numerically similar to the protection observed on the RNA level (51%) and a marked improvement (p = 0.005) over the ∼30% protection provided with control IgG NPs.

DISCUSSION

This paper reports on the development of a novel dual bioactive NP formulation for targeted delivery of antioxidant and anti-inflammatory cargoes. Taking advantage of the interactions between TP and MnTMPyP, the NPs are formed spontaneously via a controlled precipitation mechanism in the presence of a surfactant, such as PF127. The ion-pairing mechanism of NP formation using water-soluble precursor compounds obviates the need for organic solvents or external energy that could potentially affect the stability of the pharmacophores. Further, since the two active compounds serve as the NP matrix material, a high drug payload enables the use of a lower formulation therapeutic dose.

There was a clear correlation between the amount of MnTMPyP added and the amounts of MnTMPyP and TP incorporated into particles. The incorporation of the additional particle-forming ion-pair complex was not accompanied by an increase in the particle size. In fact, the effective diameter of the resultant NP was shown to decrease with higher MnTMPyP formulation amounts, up to a certain concentration. This was likely due to the increasing engagement of TP, initially present in a large excess, in the formation of the ion-pair complex, thus reducing the net surface charge coming from unneutralized phosphate groups and allowing for more effective binding of the hydrophobic block of the nonionic PF-127.

Considering that the percent drug added is roughly equivalent for the two compounds, and the amount of TP added is ∼5 times that of MnTMPyP on a molar basis, we can presume that 5 molecules of TP are associated with each MnTMPyP molecule. With a +5 charge for the MnTMPyP and a −2 charge for the TP (when both are in their free form), this

dx.doi.org/10.1021/mp400677y | Mol. Pharmaceutics 2014, 11, 2262−2270

is not the ratio that would be expected for the ion-pair complex formed with complete mutual displacement of the respective counterions. However, based on steric effects, it may be impossible for each TP molecule to associate with multiple sites on a given MnTMPyP molecule or even on neighboring MnTMPyP molecules. It is noteworthy that this complex stoichiometry appears to be particularly stable, as suggested by the similar MnTMPyP:TP ratios observed for all studied MnTMPyP formulation amounts (compare Figures 2A and 2B).

The results observed in studies considering the effect of surfactant on size and drug loading were somewhat surprising. Increasing or decreasing the PF127 concentration in the range of 5−20% had little effect on size or drug loading. This implies that the particle structure is primarily based on the structure of the core material with the PF127 there to provide surface stabilization and a means of adding targeting agents. Switching to TPGS, which would be expected to align better with the TP, resulted in a significant decrease in drug incorporation. Evidently, instead of improving stabilization, it impaired association of the TP and MnTMPγP.

Having chosen a preferred formulation (50 mg/mL MnTMPyP, 10% PF127), further studies were performed to characterize the NPs. The SOD-like activity of MnTMPyP was similar in intact and EDTA-disrupted NPs. Considering that superoxide is charged and does not pass easily through lipid membranes, the maintained activity in intact NPs indicates that MnTMPyP may be oriented toward the surface of the NPs in order to remain accessible. Alternatively, in contrast to nonionic lipids, the polar ion-pair complex may provide sufficient diffusivity for superoxide to access the porphyrins in the particle core, especially considering the slight linearly changing dimensions of the particles.

Binding of antibodies to the NPs was also found to increase linearly with the amount of MnTMPyP added. This would agree with the idea that, as additional MnTMPyP is added, the overall number of particles increases. Overall, it appears that ∼120 Abs can be added per particle when aiming for 200. Although not surprising that the two conjugation chemistries (SA−biotin and SATA−maleimide) produced similar results, this is an important confirmation. While SA−biotin is known to be a high affinity linkage, it may have limited clinical applicability due to the potential immunogenicity of streptavidin.

Drug release and size stability were evaluated at 37 °C in one of two diluents: PB or PBS. Although a nonsalinized solution is not physiologically relevant, it was valuable to see what contribution this was making to drug release. NaCl may break up the electrostatic interactions present in the NPs, leading to particle breakdown. As particle formation is dependent on interaction of TP and MnTMPyP, it was presumed that release of TP would mirror that of MnTMPyP and so only that was monitored. Drug release was quite slow in PB alone, reaching only 80% remaining at 24 h. However, although accelerated with the addition of saline, drug release was still quite slow with virtually no initial burst release. In fact, this release profile may be better suited for the treatment of acute conditions that need rapid therapy. The maintenance of size throughout the study period indicates that particles do not gradually erode but instead degrade entirely, reducing the overall number of NPs and releasing drug in that manner.

The enhanced targeting of anti-PECAM coated NPs boosted the protective potency. Targeted NPs exhibited nearly 4-fold enhanced binding over control IgG NPs. Protection against upregulation of inflammatory markers was also observed on both the RNA and protein levels. Future studies should evaluate the effect of these NPs in vivo as well as seek to elucidate the role of the drug combination in achieving a therapeutic effect.

This study is a valuable addition to the literature studying this novel NP formulation based on spontaneous coprecipitation of oppositely charged water-soluble precursor compounds and employing extremely mild, aqueous conditions. Previously, this method was used for incorporation and guided delivery of chemically labile biotherapeutics, including antioxidant enzymes[30] and gene vectors.[31] In the present study, this approach was successfully adapted and applied for encapsulation and targeting of small molecule agents. Notably, the metal porphyrin compound, which is susceptible to inactivation,[32,33] provides an example of a pharmacophore whose stability and functionality can be effectively preserved using this solventless, spontaneous formulation strategy as demonstrated here.

The noncovalent drug complex design of this formulation is also noteworthy as it offers considerable flexibility and does not require chemical modification of the pharmacophores yet also provides the mutual change in the organo-/hydrophilicity required for configuring their complex in colloidally stable nanocarriers. The PEGylated surface of these particles coated with PF-127, in addition to being essential for "stealth" properties, is also amenable for attachment of affinity ligands, thus greatly extending the range of potential clinical applications.

Importantly, while this design is not readily applicable to any pair of pharmacologically complementary pharmacophores, it can potentially provide a convenient and effective strategy for nanoencapsulation and targeted delivery of a large number of amphiphilic and hydrophobic agents, either as part of the ion-pair complex or through physical entrapment in the particle core. It would be interesting to evaluate what requirements are necessary for formation of NPs—for example, a basal colloidal structure as might be expected with TP—and, therefore, how far this technology could be expanded. One possible limitation in using bioactive compounds as the NP matrix material is an inability to control the drug ratio to the same extent as could be done when the compounds are simply being loaded. However, this may be outweighed by the potential advantages, such as capacity for a high therapeutic payload, slow drug release, or reduced toxicity.

■ CONCLUSIONS

Based on the role of oxidative stress in inflammation, a novel antioxidant/anti-inflammatory NP was designed. Capitalizing on the interactions of TP and MnTMPyP, NPs could be formed with only the addition of surfactant. The size, drug incorporation efficiency, and antibody surface coating were shown to be dependent on the amount of MnTMPyP added as well as the choice of surfactant. MnTMPyP was shown to retain its SOD-like activity while in intact particles and to release in a slow and controlled manner. Preliminary in vitro studies confirmed enhanced targeting and reduced VCAM upregulation of the anti-PECAM NPs over control IgG NPs.

■ ASSOCIATED CONTENT

Supporting Information

Supplementary schemes and figures. This material is available free of charge via the Internet at http://pubs.acs.org.

AUTHOR INFORMATION

Corresponding Author

*University of Pennsylvania, Perelman School of Medicine, Department of Pharmacology and Center for Targeted Therapeutics and Translational Nanomedicine, TRC10-125, 3400 Civic Center Boulevard, Philadelphia, PA 19104, United States. Tel: +1-215-898-9823. Fax: +1-215-573-9135. E-mail: muzykant@mail.med.upenn.edu.

Notes

The authors declare no competing financial interest.

ACKNOWLEDGMENTS

M.D.H. acknowledges financial support from the University of Pennsylvania Hematology T32 Training Grant (Grant No. T32 HL07439). This study was in part supported by the NIH Grant HL087036 (V.M.).

REFERENCES

(1) Zhang, Y.; Schwerbrock, N. M. J.; Rogers, A. B.; Kim, W. Y.; Huang, L., Codelivery of VEGF siRNA and Gemcitabine Monophosphate in a Single Nanoparticle Formulation for Effective Treatment of NSCLC. *Mol. Ther.* **2013**.

(2) Bae, Y.; Alani, A.; Rockich, N.; Lai, T.; Kwon, G. Mixed pH-sensitive polymeric micelles for combination drug delivery. *Pharm. Res.* **2010**, *27*, 2421−2432.

(3) Wei, W.; Lv, P.-P.; Chen, X.-M.; Yue, Z.-G.; Fu, Q.; Liu, S.-Y.; Yue, H.; Ma, G.-H. Codelivery of mTERT siRNA and paclitaxel by chitosan-based nanoparticles promoted synergistic tumor suppression. *Biomaterials* **2013**, *34*, 3912−3923.

(4) Muzykantov, V. R. Delivery of antioxidant enzyme proteins to the lung. *Antioxid. Redox. Signaling* **2001**, *3*, 39−62.

(5) Christofidou-Solomidou, M.; Muzykantov, V. R. Antioxidant Strategies in Respiratory Medicine. *Treat. Respir. Med.* **2006**, *5*, 47−78.

(6) Han, J.; Shuvaev, V. V.; Muzykantov, V. R. Targeted interception of signaling reactive oxygen species in the vascular endothelium. *Ther. Delivery* **2012**, *3*, 263−276.

(7) Muzykantov, V. R. Biomedical aspects of targeted delivery of drugs to pulmonary endothelium. *Exp. Opin. Drug Delivery* **2005**, *2*, 909−926.

(8) Muro, S.; Muzykantov, V. R. Targeting of Antioxidant and Anti-Thrombotic Drugs to Endothelial Cell Adhesion Molecules. *Curr. Pharm. Des.* **2005**, *11*, 2383−2401.

(9) Shuvaev, V. V.; Tliba, S.; Pick, J.; Arguiri, E.; Christofidou-Solomidou, M.; Albelda, S. M.; Muzykantov, V. R. Modulation of endothelial targeting by size of antibody-antioxidant enzyme conjugates. *J. Controlled Release* **2011**, *149*, 236−241.

(10) Simone, E.; Ding, B.-S.; Muzykantov, V. Targeted delivery of therapeutics to endothelium. *Cell Tissue Res.* **2009**, *335*, 283−300.

(11) Thomas, S. R.; Witting, P. K.; Drummond, G. R. Redox control of endothelial function and dysfunction: molecular mechanisms and therapeutic opportunities. *Antioxid. Redox Signaling* **2008**, *10*, 1713−1765.

(12) Guzik, T. J.; Harrison, D. G. Vascular NADPH oxidases as drug targets for novel antioxidant strategies. *Drug Discovery Today* **2006**, *11*, 524−533.

(13) Shuvaev, V. V.; Han, J.; Yu, K. J.; Huang, S.; Hawkins, B. J.; Madesh, M.; Nakada, M.; Muzykantov, V. R. PECAM-targeted delivery of SOD inhibits endothelial inflammatory response. *FASEB J.* **2011**, *25*, 348−57.

(14) Han, J.; Shuvaev, V. V.; Muzykantov, V. R. Catalase and Superoxide Dismutase Conjugated with Platelet-Endothelial Cell Adhesion Molecule Antibody Distinctly Alleviate Abnormal Endothelial Permeability Caused by Exogenous Reactive Oxygen Species and Vascular Endothelial Growth Factor. *J. Pharmacol. Exp. Ther.* **2011**, *338*, 82−91.

(15) Ding, B.-S.; Hong, N.; Christofidou-Solomidou, M.; Gottstein, C.; Albelda, S. M.; Cines, D. B.; Fisher, A. B.; Muzykantov, V. R. Anchoring Fusion Thrombomodulin to the Endothelial Lumen Protects against Injury-induced Lung Thrombosis and Inflammation. *Am. J. Respir. Crit. Care Med.* **2009**, *180*, 247−256.

(16) Shuvaev, V. V.; Muzykantov, V. R. Targeted modulation of reactive oxygen species in the vascular endothelium. *J. Controlled Release* **2011**, *153*, 56−63.

(17) Liang, H. L.; Hilton, G.; Mortensen, J.; Regner, K.; Johnson, C. P.; Nilakantan, V. MnTMPyP, a cell-permeant SOD mimetic, reduces oxidative stress and apoptosis following renal ischemia-reperfusion. *Am. J. Physiol.* **2009**, *296*, F266−F276.

(18) Seija, M.; Baccino, C.; Nin, N.; Sánchez-Rodríguez, C.; Granados, R.; Ferruelo, A.; Martínez-Caro, L.; Ruíz-Cabello, J.; de Paula, M.; Noboa, O.; Esteban, A.; Lorente, J. Á. Role of Peroxynitrite in Sepsis-Induced Acute Kidney Injury in an Experimental Model of Sepsis in Rats. *Shock* **2012**, 38.

(19) Libinaki, R.; Tesanovic, S.; Heal, A.; Nikolovski, B.; Vinh, A.; Widdop, R. E.; Gaspari, T. A.; Devaraj, S.; Ogru, E. Effect of tocopheryl phosphate on key biomarkers of inflammation: Implication in the reduction of atherosclerosis progression in a hypercholesterolaemic rabbit model. *Clin. Exp. Pharmacol. Physiol.* **2010**, *37*, 587−592.

(20) Zingg, J.-M.; Libinaki, R.; Lai, C.-Q.; Meydani, M.; Gianello, R.; Ogru, E.; Azzi, A. Modulation of gene expression by α-tocopherol and α-tocopheryl phosphate in THP-1 monocytes. *Free Radical Biol. Med.* **2010**, *49*, 1989−2000.

(21) Ogru, E.; Libinaki, R.; Gianello, R.; West, S.; Munteanu, A.; Zingg, J.-M.; Azzi, A. Modulation of Cell Proliferation and Gene Expression by α-Tocopheryl Phosphates: Relevance to Atherosclerosis and Inflammation. *Ann. N.Y. Acad. Sci.* **2004**, *1031*, 405−411.

(22) Newman, P. J. The biology of PECAM-1. *J. Clin. Invest.* **1997**, *99*, 3−8.

(23) Muro, S.; Wiewrodt, R.; Thomas, A.; Koniaris, L.; Albelda, S. M.; Muzykantov, V. R.; Koval, M. A novel endocytic pathway induced by clustering endothelial ICAM-1 or PECAM-1. *J. Cell Sci.* **2003**, *116*, 1599−1609.

(24) Muzykantov, V. R.; Christofidou-Solomidou, M.; Balyasnikova, I.; Harshaw, D. W.; Schultz, L.; Fisher, A. B.; Albelda, S. M. Streptavidin facilitates internalization and pulmonary targeting of an anti-endothelial cell antibody (platelet-endothelial cell adhesion molecule 1): A strategy for vascular immunotargeting of drugs. *Proc. Natl. Acad. Sci. U.S.A.* **1999**, *96*, 2379−2384.

(25) Scherpereel, A.; Rome, J. J.; Wiewrodt, R.; Watkins, S. C.; Harshaw, D. W.; Alder, S.; Christofidou-Solomidou, M.; Haut, E.; Murciano, J.-C.; Nakada, M.; Albelda, S. M.; Muzykantov, V. R. Platelet-Endothelial Cell Adhesion Molecule-1-Directed Immunotargeting to Cardiopulmonary Vasculature. *J. Pharmacol. Exp. Ther.* **2002**, *300*, 777−786.

(26) Dziubla, T. D.; Shuvaev, V. V.; Hong, N. K.; Hawkins, B. J.; Madesh, M.; Takano, H.; Simone, E.; Nakada, M. T.; Fisher, A.; Albelda, S. M.; Muzykantov, V. R. Endothelial targeting of semi-permeable polymer nanocarriers for enzyme therapies. *Biomaterials* **2008**, *29*, 215−227.

(27) Ding, B.-S.; Gottstein, C.; Grunow, A.; Kuo, A.; Ganguly, K.; Albelda, S. M.; Cines, D. B.; Muzykantov, V. R. Endothelial targeting of a recombinant construct fusing a PECAM-1 single-chain variable antibody fragment (scFv) with prourokinase facilitates prophylactic thrombolysis in the pulmonary vasculature. *Blood* **2005**, *106*, 4191−4198.

(28) Partridge, J.; Carlsen, H.; Enesa, K.; Chaudhury, H.; Zakkar, M.; Luong, L.; Kinderlerer, A.; Johns, M.; Blomhoff, R.; Mason, J. C.; Haskard, D. O.; Evans, P. C. Laminar shear stress acts as a switch to regulate divergent functions of NF-κB in endothelial cells. *FASEB J.* **2007**, *21*, 3553−3561.

(29) Schmittgen, T. D.; Livak, K. J. Analyzing real-time PCR data by the comparative CT method. *Nat. Protoc.* **2008**, *3*, 1101−1108.

(30) Chorny, M.; Hood, E.; Levy, R. J.; Muzykantov, V. R. Endothelial delivery of antioxidant enzymes loaded into non-polymeric magnetic nanoparticles. *J. Controlled Release* **2010**, *146*, 144−151.

(31) Chorny, M.; Fishbein, I.; Tengood, J. E.; Adamo, R. F.; Alferiev, I. S.; Levy, R. J. Site-specific gene delivery to stented arteries using magnetically guided zinc oleate-based nanoparticles loaded with adenoviral vectors. *FASEB J.* **2013**, *27*, 2198−2206.
(32) Dwyer, B. E.; Lu, S.-Y.; Laitinen, J. T.; Nishimura, R. N. Protective Properties of Tin- and Manganese-Centered Porphyrins Against Hydrogen Peroxide-Mediated Injury in Rat Astroglial Cells. *J. Neurochem.* **1998**, *71*, 2497−2504.
(33) Batinic-Haberle, I.; Reboucas, J. S.; Spasojevic, I. Superoxide dismutase mimics: chemistry, pharmacology, and therapeutic potential. *Antioxid. Redox Signaling* **2010**, *13*, 877−918.